

Interfacial superconductivity in bilayer and multilayer IV–VI semiconductor heterostructures

O. I. Yuzepovich^{a)}

B. Verkin Institute for Low Temperature Physics and Engineering, National Academy of Sciences of Ukraine, pr. Lenina 47, Kharkov 61103, Ukraine; Solid State Institute, Technion, 32100 Haifa, Israel; International Laboratory of High Magnetic Fields and Low Temperatures, 95 Gajowicka St., 53-421 Wrocław, Poland

M. Yu. Mikhailov

B. Verkin Institute for Low Temperature Physics and Engineering, National Academy of Sciences of Ukraine, pr. Lenina 47, Kharkov 61103, Ukraine

S. V. Bengus

B. Verkin Institute for Low Temperature Physics and Engineering, National Academy of Sciences of Ukraine, pr. Lenina 47, Kharkov 61103, Ukraine; International Laboratory of High Magnetic Fields and Low Temperatures, 95 Gajowicka St., 53-421 Wrocław, Poland

A. Yu. Aladyskin, E. E. Pestov, and Yu. N. Nozdrin

Institute for Physics of Microstructures of the Russian Academy of Sciences, Nizhniĭ Novgorod, GSP-105, 603950, Russia

A. Yu. Sipatov

National Technical University “Kharkov Polytechnical Institute,” ul. Frunze 21, Kharkov 61002, Ukraine

E. I. Buchstab and N. Ya. Fogel

Solid State Institute, Technion, 32100 Haifa, Israel

(Submitted August 13, 2008)

Fiz. Nizk. Temp. **34**, 1249–1258 (December 2008)

A comprehensive investigation and comparison of the superconducting properties of bilayer and multilayer epitaxial heterostructures of IV–VI semiconductors exhibiting superconductivity at critical temperatures $T_c \leq 6.5$ K is carried out. The superconductivity of these systems is due to inversion of the bands in the narrow-gap semiconductors on account of the nonuniform stresses created by the grids of misfit dislocations arising at the interfaces during the epitaxial growth. It is found that T_c and the character of the superconducting transition of bilayer PbTe/PbS heterostructures depend on the thickness d of the semiconductor layers and are directly related to the quality of the grids of misfit dislocations at the interfaces (the number and type of structural defects in the grids). Substantial differences in the behavior of bilayer sandwiches and superlattices are found. The minimum thickness d at which superconductivity appears is several times larger for bilayer than for multilayer systems. The upper critical magnetic fields H_{c2} of the bilayer systems are more anisotropic. For superlattices 3D behavior is observed in the temperature region close to T_c , and with decreasing temperature a 3D–2D crossover occurs. For the bilayer structures 2D behavior starts immediately from T_c , and a 2D–1D crossover is observed, with the sharp divergence of H_{c2} that is characteristic of superconducting nets.

© 2008 American Institute of Physics. [DOI: [10.1063/1.3029751](https://doi.org/10.1063/1.3029751)]

I. INTRODUCTION

The study of nanosize systems, with their fundamentally new physical properties, is a dynamically developing research field. Often it is necessary to use rather complicated technology to create nanostructure objects. However, it is possible to make nanostructures by simpler means—by the method of self-organization. In this paper we discuss superconducting nanostructures which are self-organizing at the interfaces of IV–VI semiconductor heterostructures.

The heterostructures studied are epitaxially grown superlattices (SLs) and bilayer sandwiches consisting of two semiconductor materials, from groups IV and VI, with different

periods of the crystal lattice. The “joining” of the crystal lattices of the semiconductors occurs through the formation of a periodic grid of misfit dislocations at the interface. Superconductivity itself is an unusual property of such objects, since the individual semiconductor films making up the heterostructure are not superconductors. The superconductivity of multilayer semiconductor heterostructures (PbTe/PbS and PbTe/SnTe superlattices) was discovered back in the 1980s,^{1,2} but its nature remained unclear for a long time. Several hypotheses have been advanced to explain it: the formation of an ultrathin film of lead at the interface, or Pb segregations due to interdiffusion;¹ the influence of pseudo-

morphic growth conditions on the interface;³ the influence of the grids of edge misfit dislocations (EMDs) arising at the interface between the two semiconductors.^{2,4} Attempts to create bilayer superconducting heterostructures have been unsuccessful.^{5,6} It was concluded^{5,6} that the minimum unit exhibiting superconducting properties is a three-layer sandwich.

In Refs. 7 and 8 the influence of the structural characteristics of SLs on their superconductivity was investigated in detail, and a clear correlation was established between the superconducting properties, on the one hand, and the presence of a grid of EMDs arising at the interface during epitaxial growth of the heterostructure and the dislocation structure (the continuity of the dislocation grid and the density of dislocations), on the other. Taking this into account along with the experimental fact that chalcogenides PbTe, PbSe, and PbS become metals at hydrostatic pressures above 10 kbar and go into a superconducting state at $T \approx 6$ K (see, e.g., Refs. 9 and 10), a theoretical model explaining the nature of the superconductivity in IV–VI heterostructures was constructed in Ref. 11. It was shown that the elastic strain and the change of volume along the dislocation lines create a pressure sufficient for band inversion. Thus a conducting (superconducting) nanogrid is formed at the interface, with characteristic dimensions that are set by the grid of misfit dislocations and depend on the lattice parameters of the semiconductors of which the heterostructure is made. The period of the nanogrid for IV–VI heterostructures can vary in the interval 3–25 nm.

Based on the conclusions of the theoretical model¹¹ and the results of a comparison of the structural studies with the data of resistive measurements, the main conditions necessary for metallization of the interface, which serve as a prerequisite for the possibility of superconductivity arising in a IV–VI semiconductor superlattice, were determined. The first of these conditions is that at least one of the semiconductors of the heterostructure must be narrow-gap, with a strong pressure dependence of the energy gap. The second condition is that a grid of EMDs must exist at the interfaces of the heterostructure. As a result, superconductivity was found in five new superconducting SLs: PbS/PbSe, PbTe/PbSe, PbS/YbS, PbTe/YbS, and PbSe/EuS.¹¹ Besides, it was concluded on the basis of the theoretical model that no obstacles should exist for the appearance of superconductivity in *bilayer* heterostructures as well. Therefore, after systematically selecting the parameters of the semiconductors, we were successful in discovering superconductivity in bilayer sandwiches of PbTe/PbS, PbTe/PbSe, and PbTe/YbS.¹²

The observation of superconductivity in bilayer heterostructures raised additional questions: Why did it take so long to find superconductivity in bilayer sandwiches? Are the structural properties of the EMD grid (and, hence, the superconducting properties) observed in bilayer structures different from those of superlattices? Preliminary experimental results suggested that such differences do exist.^{11,12} For comparison of the properties of bilayer heterostructures and SLs we have undertaken a comprehensive investigation of the superconducting and structural properties of a large number of heterosystems with different numbers of semiconduc-

tor layers and different layer thicknesses. In this comparison we have also used the results obtained previously for SLs.¹¹ In addition to the standard resistive method of studying the superconducting properties of the samples we used a local microwave method that permits contactless registration of the critical temperature of superconductors.^{13,14}

II. EXPERIMENTAL TECHNIQUES

A. Techniques of sample preparation and structural studies

More than 50 bilayer heterostructures and SLs were investigated: thin semiconductor films; symmetric bilayer heterostructures of PbTe/PbS, PbTe/PbSe, and PbTe/YbS, with layer thicknesses $d_1 = d_2 = 40\text{--}300$ nm; three-layer sandwiches, symmetric and asymmetric SLs with layer thicknesses of 10–300 nm.

The epitaxial semiconductor heterostructures were prepared using chalcogenides of lead (PbTe, PbS, PbSe) and a rare-earth metal (YbS). The lead chalcogenides are narrow-gap semiconductors (band gap $E_g \leq 0.3$ eV at a temperature of 4.2 K), while YbS is a wide-gap material ($E_g = 1.7$ eV). These semiconductors have the NaCl lattice with a slight mismatch of the unit cell parameters, and during the epitaxial growth of the heterostructures the relaxation of the pseudomorphic strains occurs through the formation of a grid of EMDs at the interface.

All of the heterostructures studied were formed by the successive condensation of vapors of the corresponding semiconductors on a substrate heated to 520–570 K in an oil-free vacuum of 10^{-6} torr. The layer thicknesses and the rate of deposition were monitored *in situ* by means of a quartz crystal oscillator. The lead chalcogenides were obtained by thermal evaporation from tungsten boats, and the YbS by means of electron-beam evaporation. Only stoichiometric targets were used in the sample preparation. The substrates were freshly cleaved (001) surfaces of single-crystal KCl.

The structural studies were performed using a PÉM-U transmission microscope with a resolution of 2 Å and a DRON-3 x-ray diffractometer.

For the structural analysis we prepared a special series of PbTe/PbS samples: the first layer on the KCl substrate for all the samples was a PbS layer 40 nm thick. The thickness of the upper PbTe layer varied.

The growth of the heterostructures took place by the Frank-van der Merwe mechanism. In the initial stages of growth a pseudomorphic state was observed, i.e., the first layer repeats the structure of the layer beneath it, with the same lattice parameters. This leads to a build-up of elastic energy, which increases with the thickness of the upper layer. Relaxation of the elastic strains occurs through the formation of a regular square grid of edge misfit dislocations. The dislocation grid consists of two dislocation walls with mutually orthogonal Burgers vectors of the type $a/2$ [110]. The presence of the grid of EMDs is confirmed by the results of the transmission electron microscope studies (Fig. 1).

Upon reaching a certain critical thickness d_c ($d_c = 1$ nm for the PbS/PbTe system) the first individual islands of a regular grid of misfit dislocations appear (Fig. 1a; see also Ref. 15); further increase of the thickness leads to enlargement of the islands (Fig. 1b) and their subsequent merging

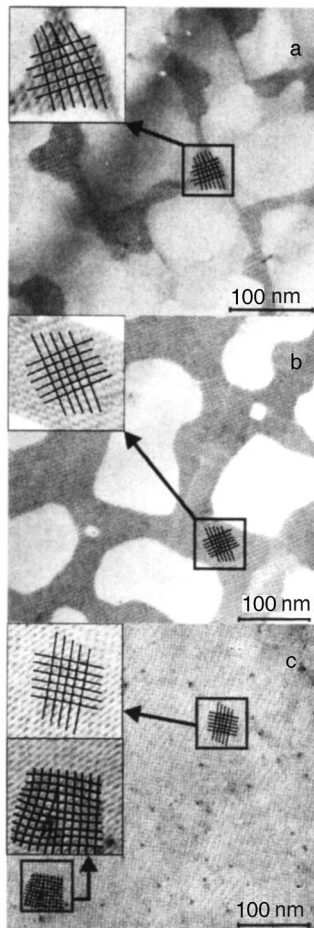


FIG. 1. Electron microscope image of PbTe–PbS/KCl bilayer heterostructures with PbTe layer thicknesses [nm]: 1 (a), 3 (b), and 30 (c). The thickness of the PbS layer is 40 nm.

into a continuous grid of misfit dislocations. At still greater thicknesses a continuous square grid of EMDs covers the entire interface, but it can have some local defects, e.g., irregularities of the periodicity (Fig. 1c).

X-ray structural analysis of many bilayer sandwiches and SLs was done in a reflection mode in a double crystal spectrometer arrangement in Cu K_{α} radiation ($\lambda = 0.154051$ nm) with $\theta - 2\theta$ scanning (see, e.g., Fig. 2). The diffractograms were taken in the (400) reflection from a sili-

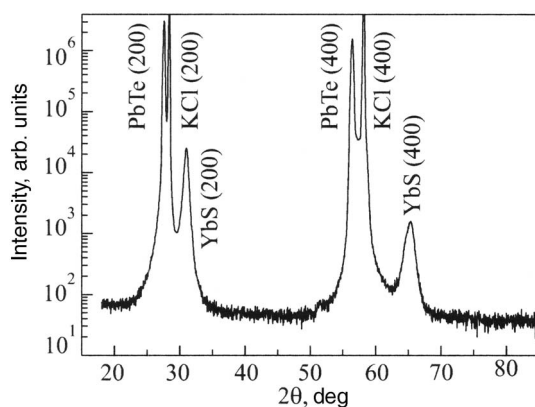


FIG. 2. X-ray diffractogram of a PbTe/YbS bilayer heterostructure with $d_{1,2} = 100$ nm.

con monochromator crystal. The diffractograms of heterostructures containing PbS sometimes showed weak reflections corresponding to free lead. In freshly prepared samples of PbTe/PbS the lead lines were most often absent, but this had no influence on the superconducting properties of the heterostructures. No correlations between the presence of lead and superconductivity have been found.⁷ In the superconducting heterostructures of PbTe/PbSe and PbTe/YbS the reflections corresponding to free lead were never observed.⁷ A more detailed description of the preparation and testing of the heterostructures may be found in Refs. 7, 8, 11, and 12.

B. Techniques of the transport measurements

The transport measurements were made in helium cryostats equipped with superconducting solenoids with maximal magnetic fields of 7 and 14 T, in the temperature intervals 0.3–300 and 1.4–300 K, respectively. The precision of the temperature determination and stabilization was 10^{-3} K or better in the temperature interval 0.3–4.2 K, and 0.05 K in the interval 4.2–300 K.

The resistance R was measured by the four-probe method on samples of double-cross shape. Both dc and ac (50 nA, 13 Hz) measurements were made. The direction of the transport current \mathbf{I} was parallel to the plane of the sample, with observance of the condition $\mathbf{I} \perp \mathbf{H}$. The values of the critical magnetic fields H_{c2} were determined from a comparison of the resistive transitions at the point $R = R_n/2$ (R_n is the residual resistance ahead of the superconducting transition). A more detailed account of the technique of the magnetotransport measurements is given in Ref. 11.

The cryostats had provisions for rotation of the sample in the magnetic field, with an angular accuracy of $\sim 0.1^\circ$.

C. Technique of measurements of nonlinear microwave properties

In the present study we have supplemented the transport measurements with measurements by the technique of local nonlinear microwave response of a superconductor with the use of a near-field probe with inductive coupling. A block diagram of the experimental apparatus is given in Refs. 13 and 14. This experimental apparatus permits study of the local nonlinear microwave response of the samples at the third-harmonic frequency. The frequency of the first harmonic is equal to 472 MHz. The level of parasitic signal at the third harmonic frequency is of the order of 10^{-13} W. The microwave probe is a copper wire 2 mm long and 50 μm in diameter, connecting the outer and inner conductors of a coaxial cable. A high-density ac current flows along the wire, producing a quasistatic magnetic field localized on a scale of the probe size. Upon the interaction of a strong microwave field with the sample, the third harmonic of the fundamental frequency in the spectrum of the reflected signal will contain information about the nonlinear properties of the superconductor. The near-field probe is used both to produce the microwave field and to register the response of the superconductor to electromagnetic radiation. Separation of the signals is done with the aid of a circulator. To prevent electrical contact of the probe with the sample, which would lead to

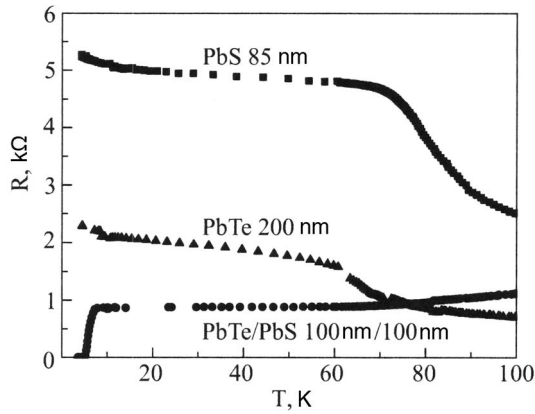


FIG. 3. Temperature dependence of the resistance of PbTe and PbS films and of a PbTe/PbS bilayer heterostructure with $d_{1,2}=100$ nm on an expanded temperature scale at zero magnetic field.

the generation of a parasitic signal at the third harmonic frequency, the sample was coated with a Teflon film $10 \mu\text{m}$ thick.

III. EXPERIMENTAL RESULTS AND DISCUSSION

A. Resistive superconducting transitions at $H=0$

Figure 3 shows the temperature dependence of the resistance for two PbTe/PbS heterostructures with $d_{1,2}=100$ nm and isolated films of PbTe and PbS (200 and 85 nm thick, respectively), prepared under the same conditions as the bilayer systems. The films do not exhibit superconductivity above 0.3 K, while the bilayer heterostructure with a single interface demonstrates a transition to a superconducting state at $T_c \approx 5.8$ K and a metallic trend of the resistance in the normal state. This radical difference in behavior of isolated films and bilayer heterostructures indicates that it is the presence of the interface between the semiconductor films that leads to metallization of the sample (the appearance of a typical metallic trend of the resistance) and to the appearance of superconductivity.

In this paper we report an experimental study and do a comparison analysis of the superconducting properties of bilayer heterosystems and PbTe/PbS superlattices with different thicknesses of the semiconductor layers. In the course of the study it is established that bilayer systems can be divided conditionally into 3 categories (although it should be noted that there are no clear boundaries between these categories). The first category consists of samples with $d \geq 80$ nm. They have a metallic type of conductivity in the normal state, with a ratio of the resistance at room temperature to that before the start of the superconducting transition $r=R_{300}/R_n$ that varies over an interval 2.1–8 and critical temperatures T_c in the interval 4.2–6.5 K (Fig. 4). The second category consists of samples with thicknesses of 50–80 nm. This is an intermediate category in which a sample in the normal state can demonstrate both metallic conductivity and conductivity of the semiconductor type but regardless of this undergo a transition to the superconducting state. The critical temperature varies in an interval of 2.3–3.3 K. The ratio $r=R_{300}/R_n$ has values in the interval 0.9–1.7. The third category consists of bilayer heterostructures with $d \leq 50$ nm. The $R(T)$ curves in the normal state for such samples are always characterized

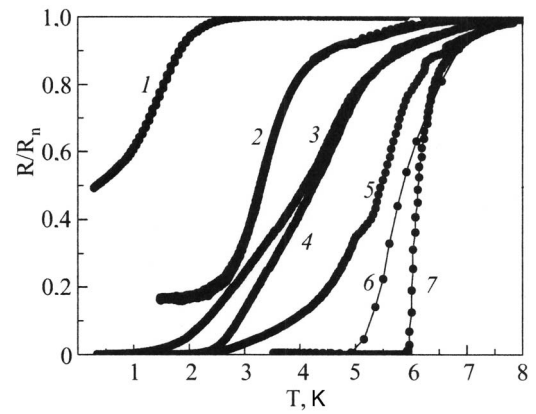


FIG. 4. Resistive transitions of PbTe/PbS bilayer heterostructures: $d_1=30$ nm, $d_2=40$ nm (1); $d_{1,2}=60$ nm (2); $d_{1,2}=70$ nm (3); $d_{1,2}=80$ nm (4); $d_{1,2}=80$ nm (5); $d_{1,2}=100$ nm (6) and for one superlattice with $d_{1,2}=120$ nm, $n=8$ (7) at zero magnetic field.

by a negative temperature coefficient of the resistance dR/dT above T_c . The resistance per square has value $R_{\square} > 1.5 \text{ k}\Omega$, and $r < 1$. For such systems T_c is often less than 1 K, and they demonstrate an uncompleted transition to the superconducting state down to the lowest temperatures at which the experiments were done (0.3 K) or else have no transition to a superconducting state at all.

In contrast to the bilayer heterostructures, all the SLs with semiconductor layer thicknesses $d \geq 10$ nm display a metallic type of conductivity in the normal state and exhibit superconductivity.¹¹

Figure 4 shows the resistive transitions for bilayer heterostructures with different semiconductor layer thicknesses and for a SL with a layer thickness $d_{1,2}=120$ nm. As we see, the resistive transitions of the bilayer systems differ from those usually observed for SLs. While for the SLs there is a sharp transition to a superconducting state (~ 0.1 K), for all the bilayer samples the transition is broadened considerably (the width of the transition can be greater than 2 K). The greater broadening of the resistive transition in the bilayer sandwiches is possibly due to the low dimensionality of the superconducting layer.

B. Superconducting transition temperatures

Figure 5 shows a plot of the superconducting transition temperature versus the semiconductor layer thickness d_{PbS} for symmetric ($d_{\text{PbS}}=d_{\text{PbTe}}$) bilayer heterostructures, trilayer sandwiches and different types of superlattices of PbTe/PbS—both symmetric and asymmetric ($d_{\text{PbS}} \neq d_{\text{PbTe}}$). For the SLs the values of T_c increase rapidly with increasing thickness from 7.5 to 20 nm. At $d_{\text{PbS}} \approx 50$ nm the critical temperature displays a tendency toward saturation. For the trilayer sandwiches the values of T_c fall into the same corridor as for the multilayer samples. The spread of experimental data for the bilayer heterostructures is significantly wider than for the SLs, although the same tendency is observed: growth of the critical temperature with increasing thickness of the semiconductor layers and a tendency toward saturation. It should be noted that the values of T_c for the bilayer sandwiches at large thicknesses, as a rule, is lower than for the case of the SLs. However, one also encounters individual bilayer sandwiches with the same values of T_c as for the SLs.

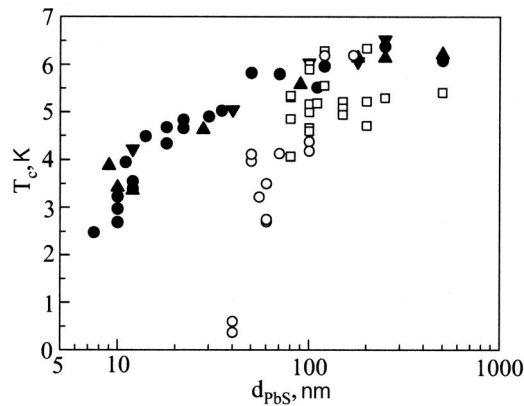


FIG. 5. Critical temperature versus semiconductor layer thickness d_{PbS} : bilayer heterostructures with an incomplete transition to the superconducting state (○), bilayer heterostructures with a complete transition to the superconducting state (□), trilayer sandwiches (▼), and symmetric $d_{\text{PbS}} = d_{\text{PbTe}}$ (●) and asymmetric $d_{\text{PbS}} \neq d_{\text{PbTe}}$ (▲) PbTe/PbS superlattices.

The essential difference between the properties of bilayer systems and SLs is the difference in the minimum layer thickness at which superconductivity appears. In the case of SLs a complete transition to the superconducting state is observed for samples with $d \geq 10$ nm, whereas for bilayer heterostructures this is true only for samples over 70 nm thick. None of the bilayer sandwiches with $d < 30$ nm shows any trace of superconductivity.

To interpret these experimental results we turn our attention to the sources of misfit dislocations and on the kinetic of formation of the EMD grids. Both of these factors have a substantial influence on the perfection (continuity and periodicity) of the dislocation grid and, accordingly, on the superconducting properties of the heterostructures. There are two sources of misfit dislocations. In the growth of the second film its free surface is the main and unlimited source of dislocations. However, a deleterious factor bearing upon the formation of a perfect grid of EMDs is the presence of dislocations formed in the growth of the first film on the substrate and which are distributed rather randomly over its surface. Therefore the original ensemble of edge misfit dislocations will be a far from perfect dislocation grid. Only when the thickness of the lower layer is greater than a certain value, viz., the thickness at which the first-mentioned source for the formation of the EMD grids is dominant, will the dislocation grids become more perfect.

The structure of the superconducting layer at the interfaces of the heterostructures reflects the structural features of the EMD grid. For the system PbTe/PbS, starting at semiconductor layer thicknesses of 1 nm, individual islands of regular EMD grids begin to appear at random places on the interface (Fig. 1a), forming an island nanostructure. Such systems belong to the third category of bilayer sandwiches and always display a semiconductor type of conductivity in the normal state. The transition to the superconducting state in these samples probably occurs owing to the presence of weak links connecting the superconducting parts. The absence of weak links at some parts of the samples will lead to an incomplete superconducting transition or to its complete absence. For samples of the intermediate category the EMD grids are more perfect and evidently comprise closed EMD-

grid regions that cover the whole interface (Fig. 1b). Conducting interfacial layers undergo a transition to the superconducting state, but in the normal state exhibit conductivity of either the metallic or semiconductor type.

A complete transition to the superconducting state and a metallic trend of the resistance in the case of bilayer heterostructures is always observed only for samples with semiconductor layer thicknesses ≥ 80 nm. Starting with that thickness the grids of misfit dislocations become rather perfect and cover the whole interface (Fig. 1c), although they may contain some local defects which do not have a strong influence on the superconducting properties of the heterostructures as a whole.

For SLs the picture is different. With the condensation of additional layers the quality of the network of EMDs on successive interfaces improves because of the decrease of the influence of the random dislocations created in the initial growth stage. This occurs even in the case of SLs with small thicknesses of the semiconductor layers. For samples containing a large number of interfaces the imperfection of the first interface is not as important and does not influence the superconducting properties of the sample as a whole. Thus for SLs the smallest thickness of the semiconductor layers for which sufficiently regular grids of EMDs appear at the interfaces and, hence, superconductivity appears amounts to about 10 nm;¹¹ these SLs have conductivity of the metallic type and exhibit a complete superconducting transition at much smaller thicknesses of the semiconductor layers.

The spread of values of the critical temperatures T_c of the bilayer heterostructures and SLs, in spite of identical growth conditions (vacuum, substrate temperature, rate of condensation), in our view, is due mainly to the presence and distribution of defects of the EMDs, which in turn may depend on the quality of the KCl substrate.

C. Upper critical magnetic field

The temperature dependence of the upper critical magnetic fields of bilayer heterostructures was studied and compared with that for the SLs. The critical magnetic fields of bilayer sandwiches are more anisotropic than those for the SLs. In superconductors near T_c one observes three-dimensional (3D) behavior of the parallel critical field, $H_{c\parallel} \sim (T_c - T)$, while at low temperatures a crossover to 2D behavior is seen (Fig. 6). A dimensional crossover of this type is observed for the majority of artificial SLs of different classes.¹⁶ A qualitative comparison of the features of the behavior of the upper critical fields with those observed for ordinary artificial SLs permits the conclusion that multilayer semiconductor heterostructures consist of superconducting layers separated by nonconducting spaces and belong to the class of superconductor-insulator superlattices.

In the case of the single interface of a bilayer structure one sees a different picture: 2D behavior of the parallel critical field ($H_{c\parallel} \sim (T_c - T)^{1/2}$), starting directly from T_c (Fig. 7). Moreover, as is seen in Fig. 7, for bilayer systems at low temperatures a crossover of the 2D-1D type is observed, with a sharp divergence of the upper critical field $H_{c\parallel}(T)$. According to the theory of Ref. 17, crossover of this type is characteristic for superconducting nanonets. It should be noted that a sharp divergence is also observed for the perpendicular

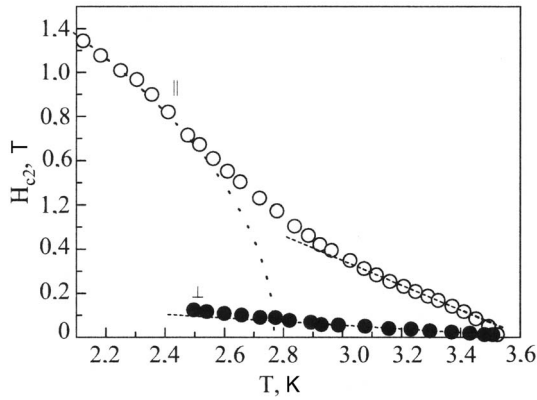


FIG. 6. Temperature dependence of the parallel and perpendicular upper critical magnetic fields for a PbTe/PbS superlattice with $d_{1,2}=18.5$ nm and $n=20$.

magnetic field, which is also characteristic of superconducting nanonets. These experimental facts are in agreement with the conclusions of our theoretical model¹¹ of a nanoscale structure of the interfacial superconducting layers in IV–VI semiconductor heterostructures.

As is seen in Fig. 7, the anisotropy of H_{c2} is very strong. The coherence length $\xi(0)$ at $T=0$, calculated from the derivative of the perpendicular critical field near T_c , lies in the range 20–40 nm for the different samples.

D. Nonlinear microwave response of the superconducting heterostructures

Figure 8 shows the temperature dependence of the power of the microwave signal at the frequency of the third harmonic, $P_{3\omega}(T)$, and the temperature dependence of the resistance for a PbTe/PbS bilayer heterostructure with a semiconductor layer thickness $d_{1,2}=200$ nm and a PbTe/PbS superlattice with $d_{1,2}=130$ nm and number of layers $n=8$. The $P_{3\omega}(T)$ curves have a pronounced maximum below the temperature of the superconducting transition in the absence of magnetic field and at low magnetic fields, as is characteristic for superconductors.^{13,14,18} Previously for superconductors (YBCO polycrystals, single crystals, thin epitaxial films, and Nb films) a correlation has been established between the temperature dependence of the nonlinear microwave re-

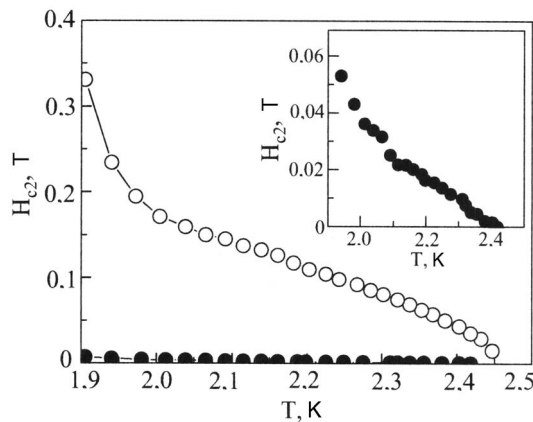


FIG. 7. Temperature dependence of the parallel and perpendicular (also in inset) upper critical fields for a PbTe/YbS bilayer heterostructure with layer thickness $d_{1,2}=100$ nm.

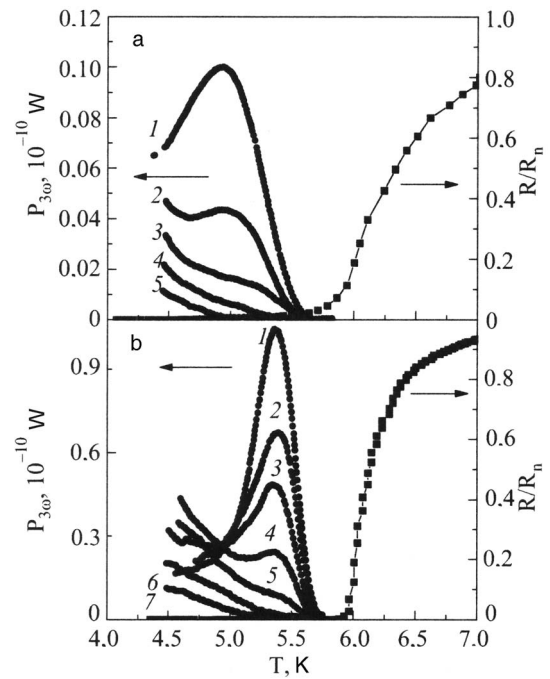


FIG. 8. Temperature dependence of the power of the third harmonic, $P_{3\omega}$, for different values of the magnetic field and the resistive transitions at zero magnetic field: a) PbTe/PbS bilayer heterostructure with $d_{1,2}=200$ nm for H [mT]: 0 (1), 1.2 (2), 2.5 (3), 3.75 (4), 15 (5); b) a PbTe/PbS superlattice with $d_{1,2}=130$ nm, $n=8$, for H [mT]: 0 (1), 1.25 (2), 1.85 (3), 2.5 (4), 3.75 (5), 6.25 (6), 27.5 (7).

sponse and the resistive transitions to the superconducting state.^{13,14,18} The presence of such a correlation makes it possible to determine T_c from the results of contactless microwave measurements. The appearance temperature of the response $P_{3\omega}(T)$ corresponds to the temperature T_{c0} at which the resistance of the sample goes to zero, and the temperature at which the maximum of the nonlinearity is reached corresponds to the temperature at which the pinning current vanishes.^{13,14} A similar correlation is also observed for the samples studied in the present work (see the $P_{3\omega}(T)$ and $R(T)$ curves in Fig. 8).

As can be seen from a comparison of Fig. 8a and 8b, the intensity of the nonlinearity peak for SLs is greater than that for bilayer heterostructures by approximately a factor of 10. This is apparently due to the presence of additional superconducting interfaces taking part in the superconductivity.

The critical temperatures of bilayer heterostructures and SLs at zero magnetic field differ insignificantly, while the position of the maximum of the nonlinearity for the bilayer heterostructures is shifted strongly to lower temperatures relative to that for SLs; this is apparently evidence of a significantly lower value of the critical current for the bilayer heterostructures in comparison with the SLs.

The temperature dependence of the nonlinear response in the case of SLs displays a rather narrow peak of the nonlinearity, whereas for bilayer heterostructures the nonlinearity peak is broader, which may be due to a stronger inhomogeneity of the superconducting layer.

It follows from the experiments that the local contactless microwave method of investigating superconducting properties confirms the presence of superconductivity in the semiconductor heterostructures and is applicable for their inves-

tigation. This method allows one to scan the surface of a heterostructure to reveal nonuniformities of the superconducting properties of different parts of the sample. Such an experiment is being planned.

IV. CONCLUSION

We have established a correlation between the structural and superconducting properties of bilayer heterostructures of PbTe/PbS with different thicknesses of the semiconductor layers. We have shown that bilayer heterostructures can be conditionally divided into 3 categories. The first category is comprised of samples with a relatively perfect grid of misfit dislocations covering the whole interface; they exhibit a metallic type of conductivity in the normal state and demonstrate a complete transition to the superconducting state. The second category contains samples in which the grid of misfit dislocations is discontinuous in places and which may have conductivity of the semiconductor or metallic type, but in either case have a transition to the superconducting state at low temperatures. The third category contains samples with an island grid of misfit dislocations, with conductivity of the semiconductor type, and these samples either have no transition to the superconducting state or demonstrate an uncompleted transition with $T_c < 1$ K.

The local microwave method, which permits contactless registration of the critical temperature of a superconductor, confirms the presence of superconductivity, observed by the resistive method, in bilayer heterostructures.

We have found substantial differences of the superconducting properties of bilayer systems from those for SLs. The minimum thickness of the semiconductor layers for which superconductivity appears is substantially smaller for the SLs than for the bilayer heterostructures. Practically all the SLs have a metallic type of conductivity and exhibit a complete superconducting transition. This is due to the circumstance that the grids of misfit dislocations on the interfaces more remote from the substrate are more perfect, even in the case of SLs with small thicknesses of the semiconductor layers. Our results imply that given attempts by other authors to detect superconductivity in bilayer IV–VI heterostructures were unsuccessful because the experiments were done on sandwiches with too small thickness of the semiconductor layers.

The intensity of the peak of the nonlinear microwave response for SLs is much higher than for bilayer heterostructures on account of the larger number of interfaces and, hence, the larger amount of superconducting material in the sample.

We have detected a difference in the character of the temperature dependence of the upper critical fields for bilayer heterostructures and SLs. The critical magnetic fields of bilayer sandwiches are more anisotropic than those for SLs. In SLs near the critical temperature one observes 3D behavior of the parallel critical field, and at low temperatures a crossover to 2D behavior occurs. In the case of the single interface in a bilayer structure one observes a different picture: 2D behavior of the parallel critical field starts directly from T_c . At low temperatures a crossover of the 2D-1D type

is observed, with a sharp divergence of the upper critical field. Crossover of this type is characteristic for superconducting nanonets.

Thus we have demonstrated differences in the superconducting properties of bilayer heterostructures and superlattices and also for bilayer heterostructures with different thicknesses of the semiconductor layers, and have shown that the main differences of the behavior of these two types of heterostructures is determined by the quality of the grids of edge misfit dislocations on the interfaces and their number. We have shown that the dimensionality and period of the self-organized superconducting nanostructures in semiconductor heterostructures can be changed by the choice of the type of semiconductors, the thickness of the semiconductor layers, and their number.

This study was supported by the Ukrainian Government Foundation for Basic Research (Grant No. F8/307-2004) and the Russian Foundation for Basic Research (Grant No. 06-02-16592). The authors thank W. Nizankowski for interest in this study and helpful discussions.

^aE-mail: yuzepovich@ilt.kharkov.ua

-
- ¹K. Murase, S. Ishida, S. Takaoka, and T. Okumura, *Surf. Sci.* **170**, 486 (1986).
 - ²O. A. Mironov, B. A. Savitskiĭ, A. Yu. Sipatov, A. I. Fedorenko, A. I. Chirkin, S. V. Chistyakov, and L. P. Shpakovskaya, *JETP Lett.* **48**, 106 (1988).
 - ³D. Agassi and T. K. Chu, *Phys. Status Solidi B* **160**, 601 (1990).
 - ⁴I. M. Dmitrenko, N. Ya. Fogel', V. G. Cherkasova, A. I. Fedorenko, and A. Yu. Sipatov, *Fiz. Nizk. Temp.* **19**, 747 (1993) [*Low Temp. Phys.* **19**, 533 (1993)].
 - ⁵O. A. Mironov, S. V. Chistyakov, I. Yu. Skrylev, V. V. Zorchenko, B. A. Savitskiĭ, A. Yu. Sipatov, and A. I. Fedorenko, *JETP Lett.* **50**, 334 (1989).
 - ⁶A. I. Fedorenko, V. V. Zorchenko, A. Yu. Sipatov, O. A. Mironov, S. V. Chistyakov, and O. N. Nashchekina, *Fiz. Tverd. Tela (St. Petersburg)* **41**, 1693 (1999) [*Phys. Solid State* **41**, 1551 (1999)].
 - ⁷N. Ya. Fogel, A. S. Pokhila, Yu. V. Bomze, A. Yu. Sipatov, A. I. Fedorenko, and R. I. Shekhter, *Phys. Rev. Lett.* **86**, 512 (2001).
 - ⁸A. I. Erenburg, N. Ya. Fogel, Yu. V. Bomze, A. Yu. Sipatov, A. I. Fedorenko, V. Langer, and M. Norell, *Fiz. Nizk. Temp.* **27**, 127 (2001) [*Low Temp. Phys.* **27**, 93 (2001), Erratum **27**, 991 (2001)].
 - ⁹N. B. Brandt, D. V. Gitsu, N. S. Popovich, V. I. Sidorov, and S. M. Chudinov, *JETP Lett.* **22**, 104 (1975).
 - ¹⁰Yu. A. Timofeev, B. V. Vinogradov, and E. N. Yakovlev, *Fiz. Tverd. Tela (Leningrad)* **23**, 2510 (1981) [*Sov. Phys. Solid State* **23**, 1474 (1981)].
 - ¹¹N. Ya. Fogel, E. I. Buchstab, Yu. V. Bomze, O. I. Yuzepovich, A. Yu. Sipatov, E. A. Pashitskii, A. Danilov, V. Langer, R. I. Shekhter, and M. Jonson, *Phys. Rev. B* **66**, 174513 (2002).
 - ¹²N. Ya. Fogel, E. I. Buchstab, Yu. V. Bomze, O. I. Yuzepovich, M. Yu. Mikhailov, A. Yu. Sipatov, E. A. Pashitskii, R. I. Shekhter, and M. Jonson, *Phys. Rev. B* **73**, 161306(R) (2006).
 - ¹³E. E. Pestov, V. V. Kurin, and Yu. N. Nozdrin, *IEEE Trans. Appl. Supercond.* **11**, 131 (2001).
 - ¹⁴A. Yu. Aladyshkin, A. A. Andronov, E. E. Pestov, Yu. N. Nozdrin, V. V. Kurin, A. M. Cucolo, R. Monaco, and M. Boffa, *Radiophys. Quantum Electron.* **46**, 109 (2003).
 - ¹⁵L. S. Palatnik and A. I. Fedorenko, *J. Cryst. Growth* **52**, 917 (1981).
 - ¹⁶B. Y. Jin and J. B. Ketterson, *Adv. Phys.* **38**, 189 (1989).
 - ¹⁷L. A. Turkevich and R. A. Klemm, *Phys. Rev. B* **19**, 2520 (1979).
 - ¹⁸Yu. N. Nozdrin, E. E. Pestov, V. V. Kurin, S. V. Baryshev, A. V. Bobyl', S. F. Karmanenko, D. A. Sakseev, and R. A. Suris, *Fiz. Tverd. Tela (St. Petersburg)* **48**, 2136 (2006) [*Phys. Solid State* **48**, 2260 (2006)].

Translated by Steve Torstveit